



Universiteit
Leiden
The Netherlands

Aria of the Dutch North Sea

Sertlek, H.O.; Sertlek H.O.

Citation

Sertlek, H. O. (2016, June 9). *Aria of the Dutch North Sea*. Retrieved from <https://hdl.handle.net/1887/40158>

Version: Not Applicable (or Unknown)

License: [Licence agreement concerning inclusion of doctoral thesis in the Institutional Repository of the University of Leiden](#)

Downloaded from: <https://hdl.handle.net/1887/40158>

Note: To cite this publication please use the final published version (if applicable).

Cover Page



Universiteit Leiden



The handle <http://hdl.handle.net/1887/40158> holds various files of this Leiden University dissertation

Author: Sertlek, Hüseyin Özkan

Title: Aria of the Dutch North Sea

Issue Date: 2016-06-09

2.2 DERIVATIONS FOR RANGE INDEPENDENT WAVEGUIDES: A DEPTH-DEPENDENT FORMULA FOR SHALLOW WATER PROPAGATION

This section is modified version of “H.Ö. Sertlek and M.A. Ainslie, A depth-dependent formula for shallow water propagation, J. Acoust. Soc. Am. 136(2), 573-582, 2014”.

Abstract: *In shallow water propagation, the sound field depends on the proximity of the receiver to the sea surface, the seabed, the source depth and the complementary source depth. While normal mode theory can predict this depth dependence, it can be computationally intensive. In this work, an analytical solution is derived in terms of the Faddeeva function by converting a normal mode sum into an integral based on a hypothetical continuum of modes. For a Pekeris waveguide, this approach provides accurate depth dependent propagation results (especially for the surface decoupling) without requiring complex calculation methods for eigenvalues and corresponding eigenfunctions.*

2.2.1. Introduction

The accurate calculation of propagation loss (PL) is needed for many acoustic problems such as sonar performance modeling, underwater acoustic communication, environmental risk assessment and oceanography. These applications can require the simulation of propagation characteristics at different ranges and depths. Propagation loss can be defined as

$$PL = 10 \log_{10} \frac{F^{-1}}{r_{ref}^2} \text{ dB re } 1 \text{ m}^2 \quad (1)$$

where F is known as the “transmission factor” [Weston,1980] or “propagation factor” [Ainslie,2010a] and r_{ref} is the reference distance, equal to 1 m. Propagation loss can be estimated with different methods such as normal modes, ray theory, parabolic equation, and flux theory. Variation of PL with range, water depth, frequency, source depth and receiver depth can be critical for determining detection ranges, isoclines for environmental risk assessment, etc. Weston introduced an energy flux approach for the calculation of depth-averaged propagation loss without tracing rays or summing normal modes, and thus applicable to large scale problems [Weston,1971]. Weston’s flux equation can be derived from ray and mode theories [Weston,1980]. In Weston’s approach, four propagation regions are described as the spherical, cylindrical spreading, mode-stripping and single mode regions. While permitting an analytical solution even for a range dependent environment [Weston,1976], Weston’s flux formulation may not provide satisfactory simulation results when the source or receiver depths are located close to each other, to the seabed or (especially) to the sea surface. [Weston,1980] addressed this weakness by deriving depth dependence using wave theory concepts, applying these to a selection of predetermined functional forms for the distribution of energy with angle, making an implicit assumption that the frequency is sufficiently high for the various depth-dependent corrections not to overlap with one another. [Harrison,2013] derived a range- and depth-correction to Weston’s flux theory that includes ray convergence terms, while neglecting the depth dependence close to source depth, complementary depth and boundaries. In the present section, a method is developed to calculate the depth dependence by deriving a generalisation of Weston’s approach that does not rely on prior knowledge of the angular energy distribution, and

is valid even when the correction terms overlap. The solution, in terms of the Faddeeva function, is derived from an incoherent normal mode sum by using some trigonometric transformations, and is valid for any angular distribution compatible with propagation from a point source in a Pekeris waveguide, and for any source-receiver depth combination. Results computed in this way for different frequencies and receiver depths are compared with results using the normal mode program KrakenC⁸. For the comparisons, a range independent test case (Scenario A2.I) from the Weston Memorial Workshop [Ainslie,2010b; Zampolli et al,2010] is used. The detailed description of this test case is given in the comparisons section.

2.2.2. Depth Dependence of Propagation Loss

The depth dependence of PL can have different characteristics due to the depth of the receiver relative to the sea surface, seabed, source depth and complementary source depth [Weston,1980]. The complementary source (z_{cs}) or receiver depth (z_{cr}) can be defined for source depth z_s (or receiver depth z_r) as

$$z_{cs,cr} = D - z_{s,r} \quad (2)$$

where

$$D = h + \Delta_W \quad (3)$$

and $\Delta_W = \frac{\rho_2/\rho_1}{k_1 \sin \theta_c}$ is the vertical wave shift and described by [Weston,1960; Weston,1994], h is water depth, ρ_2 is the density of sediment, ρ_1 is the density of sea water, k_1 is the wavenumber in the water layer and θ_c is the sediment critical angle. When PL is plotted vs z_s for a constant receiver depth, similar depth dependent properties is observed around the true receiver depth z_r as the complementary receiver depth $D - z_r$.

2.2.2.1. Derivation

By using the incoherent mode sum, the propagation factor F for an isovelocity and isodensity waveguide can be written as

$$F(z_r, z_s) = \frac{2\pi}{r} \sum_{n=1}^{\infty} \frac{\psi_n^2(z_s) \psi_n^2(z_r)}{\kappa_n} \exp(-2\delta_n r) \quad (4)$$

Here $\psi_n(z)$ is the eigenfunction

$$\psi_n(z) = A_n \sin(\gamma_n z) \quad (5)$$

where A_n is the amplitude of n th eigenfunction, γ_n is vertical wavenumber, and κ_n the horizontal wavenumber. Defining the quantity of $L_n = \int \frac{1}{\sqrt{k_1^2(z) - \kappa_n^2}} dz = \frac{r_{\text{CM}}}{2\kappa_n}$, the normalisation constant A_n^2 can be written [Tindle and Weston, 1980]

$$A_n^2 = \frac{2}{L_n} (k_1^2 - \kappa_n^2)^{-1/2} = \frac{4 \cot \theta_n}{r_{\text{CM}}} \quad (6)$$

where r_{CM} is the modal cycle distance, and θ_n is the n th mode grazing angle given by

$$\theta_n = \arcsin\left(\frac{n\lambda}{2D}\right), n = 1, 2, 3, \dots \quad (7)$$

The relation between the modal cycle distance and geometric ray cycle distance (r_{cG}) is [Tindle and Weston,1980]

$$r_{cM} = r_{cG} + 2\Delta_B \cot\theta, \quad (8)$$

where $\Delta_B = \frac{(\gamma_{1n}^2 + \gamma_{2n}^2)}{\gamma_{1n}\gamma_{2n}^2 \left(\frac{\rho_1\gamma_{2n}}{\rho_2\gamma_{1n}} + \frac{\rho_2\gamma_{1n}}{\rho_1\gamma_{2n}} \right)}$ is the vertical *beam* shift [Weston,1994] (converted from the corresponding horizontal shift stated by [Weston and Tindle,1979]) This relation can be written for isovelocity case by substituting for $r_{cG} = 2h \cot(\theta)$

$$r_{cM} = 2(h + \Delta_B) \cot\theta. \quad (9)$$

If one uses the relations of $\gamma_{1n}^2 = k_1^2 \sin^2 \theta$ and $\gamma_{2n}^2 = k_1^2 - \gamma_{1n}^2 - k_2^2$, the beam shift takes the form

$$\Delta_B = \frac{\rho_1 \rho_2 (k_1^2 - k_2^2)}{\sqrt{k_1^2 \cos^2 \theta - k_2^2} (\rho_2^2 k_1^2 \sin^2 \theta + \rho_1^2 k_1^2 \cos^2 \theta - \rho_1^2 k_2^2)} \quad (10)$$

where $k_2 = \omega/c_2$. The attenuation term in the horizontal direction is added by a perturbation approach with the contribution of a small imaginary part δ_n to κ_n [Tindle,1979]. This small imaginary part leads to an exponential attenuation with range as $\exp(-2\delta_n r)$, where δ_n can be related to the reflection coefficient of sea bottom $V(\theta)$ according to

$$\delta_n = \text{Im}\{k_1 \cos(\theta_n)\} = -\frac{\ln(|V(\theta_n)|)}{r_{cM}} \quad (11)$$

The following relations can be obtained with the relation of $\gamma_{1n} = \frac{n\pi}{D}$ in Eq.(A4) and Eq.(A5) as shown in Appendix A.

$$F(D - z_r, z_s) = F(z_r, z_s) = F(z_r, D - z_s) \quad (12)$$

This property is useful because if $F(z_r, z_s)$ is known for $0 < z_r, z_s < D/2$, Eq.(30) permits straightforward evaluation of $F(z_r, z_s)$ for $D/2 < z_r, z_s < h$. The discrete mode sum (F) can be approximated by the following integral which is denoted by F_0 ,

$$F_0(z_r, z_s) = \frac{2\pi}{r} \int_0^\infty \frac{\psi_n^2(z_s) \psi_n^2(z_r)}{\kappa_n} |V|^{\frac{2r}{r_{cM}}} dn \quad (13)$$

By this integral representation, the integer n is replaced by a continuous function of the grazing angle θ as $n \approx n(\theta)$. The variation of $n(\theta)$ versus θ can be written as

$$\frac{dn(\theta)}{d\theta} = \frac{r_{cM}}{2\pi} k_1 \sin(\theta) \quad (14)$$

However, the integrand is defined only at the discrete eigenvalues. In the following steps, this integrand will be interpolated between the eigenvalues as a continuous function of θ , thus permitting evaluation of the integral

$$F_0(z_r, z_s) = \frac{1}{r} \int_0^{\frac{\pi}{2}} A_n^4 \sin^2(\gamma_{1n} z_s) \sin^2(\gamma_{1n} z_r) r_{cM} \tan(\theta) |V|^{\frac{2r}{r_{cM}}} d\theta \quad (15)$$

where A_n and r_{cM} are given by Eq.(6) and Eq.(9). The integral can be written in the different forms by using trigonometric identities. First, using the trigonometric identity $\sin^2(\gamma_{1n} z) \equiv \frac{1}{2} - \frac{1}{2} \cos(2\gamma_{1n} z)$ for eigenfunctions, this integral becomes

$$F_0(z_r, z_s) = \frac{4}{r} \int_0^{\frac{\pi}{2}} \frac{(1 - \cos(2\gamma_{1n} z_s))(1 - \cos(2\gamma_{1n} z_r))}{r_{cM} \tan(\theta)} |V|^{\frac{2r}{r_{cM}}} d\theta \quad (16)$$

Then, changing the variable of integration to continuous grazing angle and using the trigonometric identity

$$\cos(2k_1 z_s \sin \theta) \cos(2k_1 z_r \sin \theta) = \frac{\cos(2k_1 (z_s - z_r) \sin \theta) + \cos(2k_1 (z_s + z_r) \sin \theta)}{2} \quad (17)$$

results in the following integral form for the propagation factor,

$$F_0(z_r, z_s) = \frac{4}{r} \int_0^{\frac{\pi}{2}} \frac{(1 - W(z_r, z_s, \theta))}{r_{cM} \tan \theta} |V|^{\frac{2r}{r_{cM}}} d\theta \quad (18)$$

where the term involving source and receiver depths can be written

$$W(z_r, z_s, \theta) = \cos(2k_1 z_s \sin\theta) + \cos(2k_1 z_r \sin\theta) - \frac{\cos(2k_1 \sin\theta(z_s - z_r)) + \cos(2k_1 \sin\theta(z_s + z_r))}{2} \quad (19)$$

If $W(z_r, z_s, \theta)$ were sufficiently close to zero on average, Eq. (18) would have the same form as the flux integral, which has an analytical solution in the form of an error function if the reflection loss increases linearly with angle [Ainslie, 2010a; Macpherson and Daintith, 1967]. This gives the depth-averaged propagation factor.

2.2.2.2. Reflections from the seabed

Eq.(18) can be evaluated numerically for any given seabed reflection coefficients. The possibility of analytical evaluation for special forms of the reflection coefficient is explored next.

A. *Exponential reflection coefficient*

One reflection coefficient assumption that permits an analytical evaluation of the integral is exponential reflection coefficient in the form

$$|V| = \exp(-\eta\theta^2/\tan\theta) \quad (20)$$

where η is the rate of increase with grazing angle of the sediment reflection loss [Ainslie, 2010], in nepers per radian (Np/rad). This form of reflection coefficient simplifies the derivation without requiring small angle approximation. Specifically, the propagation factor becomes

$$F_0(z_r, z_s) = \frac{4}{r} \int_0^{\theta_c} \frac{(1 - W(z_r, z_s, \theta))}{r_{\text{CM}} \tan \theta} \exp\left(-\frac{2\eta r}{r_{\text{CM}} \tan \theta} \theta^2\right) d\theta \quad (21)$$

This integral can be solved analytically for the isovelocity and isodensity case. For the isovelocity case, ray cycle distance is $r_{\text{CM}} = 2(h + \Delta_B) \cot \theta$. Then, the propagation factor becomes

$$F_0(z_r, z_s) = \frac{2}{r} \int_0^{\theta_c} \frac{(1 - W(z_r, z_s, \theta))}{h + \Delta_B} \exp\left(-\frac{\eta r}{(h + \Delta_B)} \theta^2\right) d\theta \quad (22)$$

The vertical beam shift is important for low frequencies and is itself a function of angle [Weston, 1994]. Eq. (22) can be used for low frequencies by evaluating the integral numerically. The beam shift can be ignored for higher frequencies, in which case the following equation results

$$F_0(z_r, z_s) = \frac{2}{rh} \int_0^{\theta_c} (1 - W(z_r, z_s, \theta)) \exp\left(-\frac{\eta r}{h} \theta^2\right) d\theta, \quad (23)$$

where $W(z_r, z_s, \theta)$ is the sum of cosine functions from Eq.(19). Thus, the analytical solution for the following type of integral leads an analytical solution for the propagation factor:

$$\begin{aligned}
 \Phi[Z, R, \theta_c] &= \int_0^{\theta_c} \cos(Z\theta) \exp(-R\theta^2) d\theta \\
 &= \sqrt{\frac{\pi}{R}} \frac{\exp\left(-\frac{Z^2}{4R}\right)}{4} \left(w\left(\frac{Z}{2\sqrt{R}} - i\sqrt{R}\theta_c\right) \exp\left(\left(\frac{Z}{2\sqrt{R}} - i\sqrt{R}\theta_c\right)^2\right) \right. \\
 &\quad \left. - w\left(\frac{Z}{2\sqrt{R}} + i\sqrt{R}\theta_c\right) \exp\left(\left(\frac{Z}{2\sqrt{R}} + i\sqrt{R}\theta_c\right)^2\right) \right) \quad (24)
 \end{aligned}$$

where $w(x + iy)$ is the Faddeeva function [Poppe and Wijers, 1967; Abramowitz and Stegun, 1972] which is defined as

$$w(x + iy) = \exp(-(x + iy)^2) \left(1 + \frac{2i}{\sqrt{\pi}} \int_0^{x+iy} \exp(t^2) dt \right) \quad (25)$$

and is related to the error function [Abramowitz and Stegun, 1972] according to

$$w(x + iy) = \exp(-(x + iy)^2) \left(1 + \operatorname{erf}(i(x + iy)) \right). \quad (26)$$

The analytic expression for the propagation factor for isovelocity case can be written in terms of the function $\Phi[Z, R, \theta_c]$ as

$$\begin{aligned}
 F_0(z_r, z_s) = & r^{-\frac{3}{2}} \sqrt{\frac{\pi}{\eta h}} \operatorname{erf}\left(\sqrt{\frac{\eta r}{h}} \theta_c\right) \\
 & - \left\{ \frac{2}{rh} \left[\Phi\left[2k_1 z_s, \frac{\eta r}{h}, \theta_c\right] + \Phi\left[2k_1 z_r, \frac{\eta r}{h}, \theta_c\right] \right. \right. \\
 & \left. \left. - \frac{\Phi\left[2k_1(z_s - z_r), \frac{\eta r}{h}, \theta_c\right] + \Phi\left[2k_1(z_s + z_r), \frac{\eta r}{h}, \theta_c\right]}{2} \right] \right\} \quad (27)
 \end{aligned}$$

where the first term is the error function based solution of the classic flux integral [Ainslie,2010a; Macpherson and Daintith,1967]. The term in curly parentheses describes the depth dependence for an isovelocity waveguide. In Figure 1, $\Phi[Z, R, \theta_c]$ is plotted as a function of R , a dimensionless range variable equal to $\frac{\eta r}{h}$, and a dimensionless depth variable Z that can be any one of $2k_1 z_r$, $2k_1 z_s$, $2k_1(z_r + z_s)$ and $2k_1(z_r - z_s)$. Specifically, the graph on the left shows the depth dependence of $\Phi[Z, R, \theta_c]$ for selected constant values of R , as stated in the figure legend. Similarly, the lower graph shows the range dependence of $\Phi[Z, R, \theta_c]$ for selected values of Z . The 2D contour plot (upper right panel) shows the combined R and Z dependence in a single graph. In all three graphs, the value of $\theta_c = \arccos(1500/1700) = 0.489957$ rad is used for consistency with the parameters of the selected scenario (A2.I) from Weston Memorial Workshop 2010. More detailed description of the test cases are given in the comparisons section.

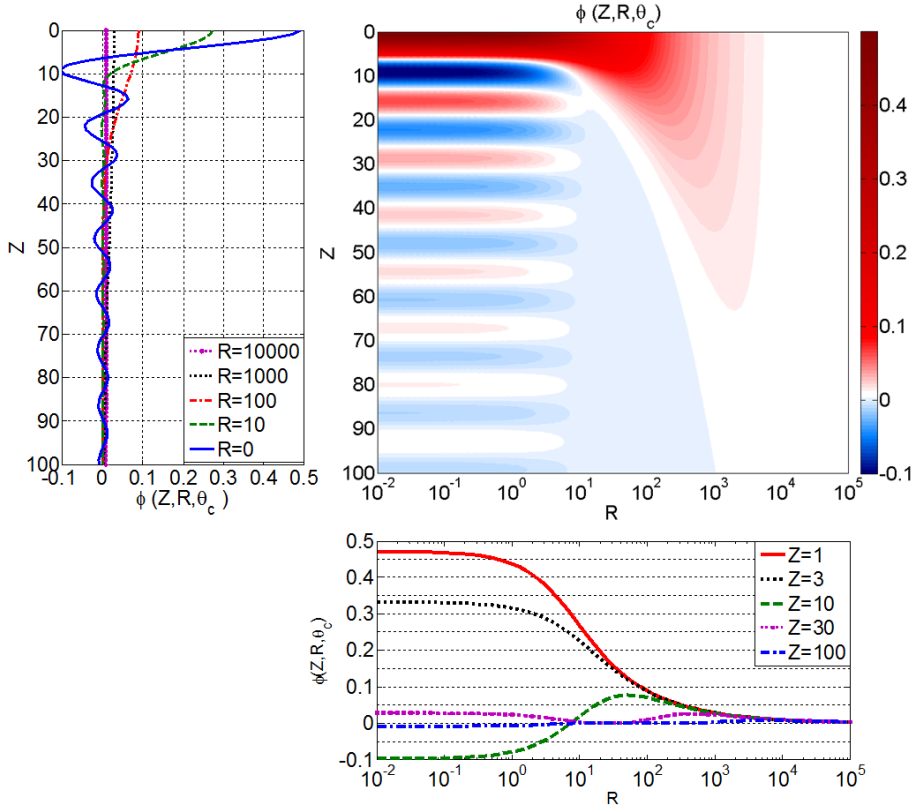


Figure 1. $\Phi[Z, R, \theta_c]$ function is plotted versus χ (on the upper left) and versus R (on the bottom right) for critical angle $\theta_c = 0.489957$ rad, corresponding to the scenario described in Sec. 2.2.3.

2D representation of $\Phi[Z, R, \theta_c]$ versus Z and R (on the upper right)

According to these figures, we expect more significant variations at low values of Z (low frequencies) and R (at small ranges or deeper water). The function $\Phi[Z, R, \theta_c]$ asymptotically approaches $\frac{1}{2} \sqrt{\frac{\pi}{R}} \exp\left(-\frac{Z^2}{4R}\right)$ for large R (by using Eq.(36)). For small R , $\lim_{R \rightarrow 0} \Phi[Z, R, \theta_c] = \frac{\sin(Z\theta_c)}{Z}$. For large Z , the asymptotic form is $\lim_{Z \rightarrow \infty} \Phi[Z, R, \theta_c] = 0$. For small Z , $\lim_{Z \rightarrow 0} \Phi[Z, R, \theta_c] = \sqrt{\pi} \frac{\text{erf}(\sqrt{R}\theta_c)}{2\sqrt{R}}$. When they are both small, $\lim_{Z, R \rightarrow 0} \Phi[Z, R, \theta_c] \approx \theta_c$. These approximate formulas can be helpful for simplifying the prediction of and increasing understanding of the dependence of the propagation on range, water depth and critical angle

B. *Harrison's approximation to Rayleigh reflection coefficient*

Use of an exponential reflection coefficient, as shown in the previous section, provides an analytical solution. This analytical solution (Eq.(27)) is based on a linear approximation to the seabed reflection loss. As it will be shown in Figure 2, the Rayleigh reflection coefficient can provide a better approximation for the decay rate [Harrison,2010]. Expressing the Rayleigh reflection coefficient in an exponential form can be computationally more efficient because of having less complicated equations in the final form. This exponential form also enables to facilitate comparisons with the previous derivations. A useful approximation to the Rayleigh reflection coefficient[Harrison,2010] that also leads to an analytical expression in a similar form to Eq.(18) is

$$|V| = \exp\left(-\frac{\eta \sin\theta}{\sqrt{1-v}\left(1 + \left(\left(\frac{\rho_2}{\rho_1}\right)^2 - 1\right)v\right)}\right) \quad (28)$$

where $v = \left(\frac{\sin\theta}{\sin\theta_c}\right)^2$, ρ_1 and ρ_2 are the densities of water and sediment. Thus, the propagation factor can be written as

$$F_0(z_r, z_s) = \frac{2}{r} \int_0^{\theta_c} \frac{(1 - W(z_r, z_s, \theta))}{(h + \Delta_B)} \exp\left(-\frac{\eta g r}{(h + \Delta_B)} \sin\theta \tan\theta\right) d\theta \quad (29)$$

where $g = \left(\sqrt{1-v}\left(1 + \left(\left(\frac{\rho_2}{\rho_1}\right)^2 - 1\right)v\right)\right)^{-1}$. In Section 2.2.3, propagation factors based on exponential and Rayleigh reflection coefficients are compared in Figure.2.

C. Symmetry of Depth Dependent Solution

The approximation F_0 is based on a continuous angle assumption for the eigenvalues as $\gamma_{1n} = k_w \sin(\theta)$. For the continuous angle approximation, the symmetry properties of propagation loss are not satisfied (See Eq.(19) and Appendix B). Therefore, the derived solution can be used to model the features at the sea surface and source depth. This derivation gives poor results for the features at sea bottom and complementary source depth as it could be seen in Figure 2. By using these symmetry properties from Eq.(A4) and Eq.(A5), the features at sea bottom and complementary source depth can be obtained from the features at sea surface and source depth as

$$F(z_r, z_s) = \begin{cases} F_-(z_r, z_s), & z_s < D/2 \\ F_+(z_r, z_s), & z_s > D/2 \end{cases} \quad (30)$$

where F_- and F_+ are defined as

$$F_-(z_r, z_s) = \begin{cases} F_0(z_r, z_s), & z_r < D/2 \\ F_0(D - z_r, z_s), & z_r > D/2 \end{cases} \quad (31)$$

and

$$F_+(z_r, z_s) = \begin{cases} F_0(z_r, D - z_s), & z_r < D/2 \\ F_0(D - z_r, D - z_s), & z_r > D/2 \end{cases} \quad (32)$$

These terms give the propagation factor (F) by using the symmetry property of source, receiver, complementary source and complementary receiver depths.

2.2.3. Comparisons

In this section, results obtained using the methods described in Sec. 2.2.2 are compared with KrakenC. In these comparisons, a range independent test case (Scenario A2.1) from the Weston Memorial Workshop [Zampolli et al,2010;Weston,1960] is used, based on Problem XI from the 2006 Reverberation Modeling Workshop at Un.Texas at Austin [Thorsos and Perkins,2007]. For Scenario A2.1, the water depth (h) is 100 m, source depth (z_s) is 30 m, sound speed in water (c_1) and sediment (c_2) are respectively are 1500 m/s and 1700 m/s, corresponding to a critical angle $\theta_c = 0.489957$ rad. The sediment-seawater density ratio (ρ_2/ρ_1) is 2 and resulting reflection loss gradient (η) is 0.273777 Np/rad, evaluated using Eq.(8.86) of [Ainslie,2010a].

[Weston,1980] derived the depth dependence for a number of specified distributions of energy with angle. For each angular distribution, which must be known in advance, four correction factors to the depth-averaged propagation factor are given of the form $[1 - f(x_0)]$ (sea surface and seabed) and $[1 + \frac{1}{2}f(x_0)]$ (source depth and complementary source depth), where $x_0 = k_1 d \phi_0$, d is the distance to the depth in question and ϕ_0 is an angle that characterises the distribution, equal to the critical angle for Weston's Case 2 ('low pass') and to the effective propagation angle $\phi_0 \approx \sqrt{\frac{h}{2\eta r}}$ for Cases 5 (Weston's 'Gaussian') and 6 ('dipole Gaussian'). In each case, the functional form $f(x_0)$ is given by Weston's Table I. In contrast to Weston's approach, use of Eq. (23) in terms of the Faddeeva function permits direct computation of the depth-dependent propagation factor without the need for prior knowledge of the angular distribution of energy. Instead, Eq.(23) and Eq.(29) automatically take into account all possible angular distribution cases for a Pekeris waveguide, dealing with transitions between different cases and combinations of multiple cases in a natural way, and permitting evaluation of all possible combinations of source or receiver depth. In Appendix C, relevant cases from Weston's table (Gaussian and dipole Gaussian) are derived from Eq.(23).

Figure 2 compares the result of evaluating expressions for Cases 2 ('low pass') and 5 ('Gaussian'). In the cylindrical spreading region (e.g., 0.5 km), the low pass solution is applicable, whereas for mode stripping (e.g., 25 km), one expects a Gaussian distribution with angle, and these expectations are confirmed by Figure 2. Less obvious is what happens for intermediate ranges (e.g., 2 km) at which it is necessary to make a choice between the low pass and Gaussian distributions. By contrast, Eq. (23) from the present section is applicable to both cylindrical spreading and mode stripping regions, including any intermediate range. Further, if greater

accuracy is required, this can be achieved by means of Harrison's approximation to the Rayleigh reflection coefficient, as implemented here in the form of our Eq. (29). For the purpose of Figure 2 and Figure 3 , to combine the effects of multiple depth correction factors from Weston's paper, we have multiplied these together in the form (denoted $F_{2,5}$ for Weston's cases 2 and 5, applicable when the source is not close to the sea surface)

$$F_{2,5} = F_{\text{ref}} \left[\left(1 + \frac{f(x_{0,z_s})}{2} \right) \left(1 + \frac{f(x_{0,z_{cs}})}{2} \right) (1 - f(x_{0,0})) (1 - f(x_{0,D})) \right] \quad (33)$$

where the second subscript of the variable x_0 indicates the depth relative to which d is measured, such that $x_{0,\zeta} = k_1(z_r - \zeta)\phi_0$. Here F_{ref} is the analytical solution of Eq.(23) for $W(z_s, z_r, \theta) = 0$ as

$$F_{\text{ref}} = r^{-\frac{3}{2}} \sqrt{\frac{\pi}{\eta h}} \text{erf} \left(\sqrt{\frac{\eta r}{h}} \theta_c \right) \quad (34)$$

In Eq. (3) of [Weston, 1980] , the low pass and Gaussian cases correspond to an assumption that $\sin^2(\gamma_{1n} z_s)$ may be replaced by its average value of 1/2. Consequently, Eq.(33) is not valid for source depths close to the sea surface or seabed on a wavelength scale. For small source depths, the depth corrections can be combined as (denoted F_6 , for Weston's case 6, 'dipole Gaussian' – as used in Figure 3)

$$F_6 = 2(k_1 z_s \phi_0)^2 F_{\text{ref}} \left[(1 - f(x_{0,0})) (1 - f(x_{0,D})) \right] \quad (35)$$

A similar form of Eq. (35) for the large receiver depth is also shown by [Denham,1986].

In Figure 2, the propagation loss results obtained with Eq.(23), Eq.(29), Weston's cases (Eq.(33)) and KrakenC are compared at different ranges. For these comparisons, Eq.(23) and Eq.(29) are evaluated numerically without applying the symmetry relations of Eqs. (30) to (32). The beam

shift is ignored in Figure 2. The classic form of the flux integral without depth dependent properties [Ainslie,2010a; Macpherson and Daintith,1967] is also plotted, as obtained by substituting $W(z_r, z_s, \theta_s) = 0$ in Eq.(23) gives this classical form of flux equation (Eq.(34)).

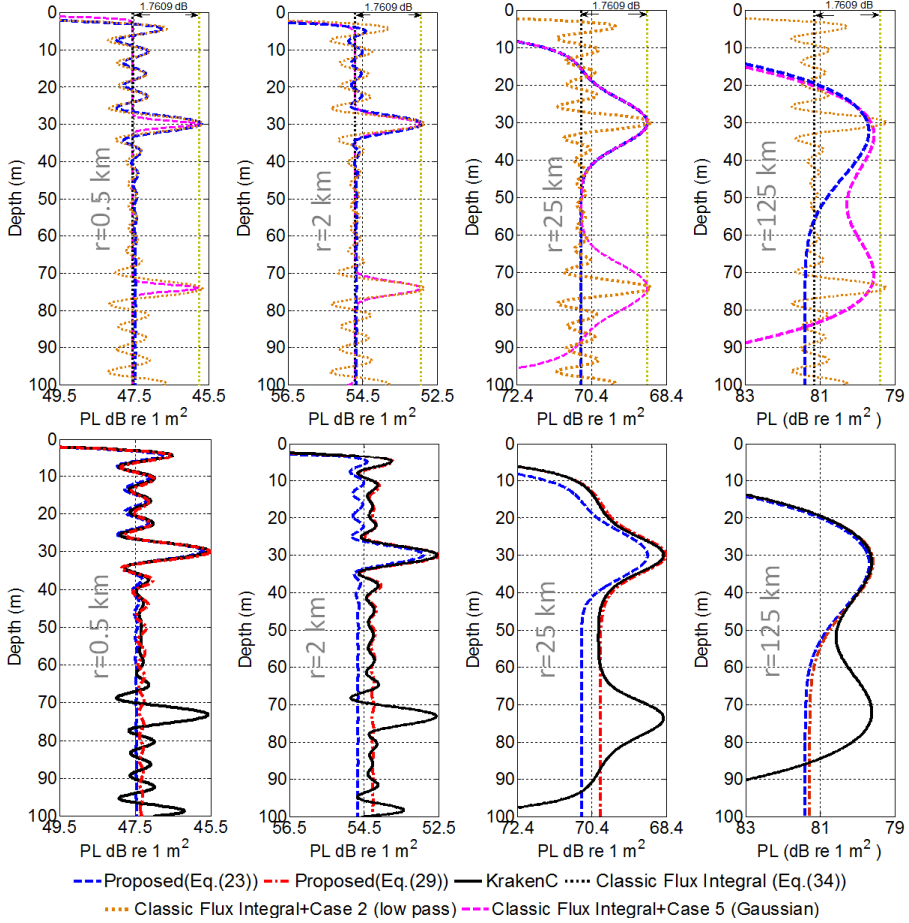


Figure 2. PL vs receiver depth calculated by Eq.(23), Weston's approach (Eq.(33)) for the various energy distributions with angle(low pass and Gaussian) and Flux integral (Eq.(34)) for 250 Hz at 0.5 km, 2 km, 25 km and 125 km.(upper graphs).PL vs receiver depth calculated by KrakenC, Eq. (23) and Eq.(29) for 250 Hz at 1 km, 5 km, 25 km and 125 km. Beam shift is neglected in these comparisons. For the dashed and dash-dotted lines, PL is approximated using $F \approx F_0$. (lower graphs) The source depth is 30 m.

The features at the complementary depth and seabed are not visible in the graphs of proposed solutions by Eq.(23) and Eq.(29) because the symmetry property of Eq.(30), Sec II.C, is not applied. They can be obtained, if desired, by applying the symmetry property described in Section 2.2.2.2.C. In Figure 3, Eq.(33) and Eq.(35) are evaluated for the different angle distributions (Gaussian and dipole Gaussian) for different source depths at 250 Hz and 25 km. In these comparisons, the same parameters of Scenario A2.I (described above) are used. The benefit of the Faddeeva function is that it includes all relevant limiting cases in one formula. To illustrate this benefit, consider the large R limit $\left(\frac{Z}{2\sqrt{R}} \ll \sqrt{R} \theta_c\right)$ in Eq.(26). In this limit, $\Phi[Z, R, \theta_c]$ simplifies to

$$\begin{aligned} \Phi[Z, R, \theta_c] &\approx \sqrt{\frac{\pi}{R}} \frac{\exp\left(-\frac{Z^2}{4R}\right)}{4} \left[(1 + \operatorname{erf}(\sqrt{R} \theta_c)) - (1 - \operatorname{erf}(\sqrt{R} \theta_c)) \right] \\ &\approx \frac{1}{2} \sqrt{\frac{\pi}{R}} \exp\left(-\frac{Z^2}{4R}\right) \end{aligned} \quad (36)$$

where $\operatorname{erf}(\sqrt{R} \theta_c) \approx 1$ for large R . When Eq. (36) is substituted in Eq.(23), we obtain the following general-purpose formula for the mode stripping region (generalising Weston's case 5 and 6)

$$F_0(z_r, z_s) = F_{\text{ref}} (1 - \exp(-2(k_1 z_r \phi_0)^2) - \exp(-2(k_1 z_s \phi_0)^2) [1 - \exp(-2(k_1 z_r \phi_0)^2)]$$

where $\phi_0 = \sqrt{\frac{h}{2\eta r}}$. The transition between Cases 5 and 6 is illustrated in Figure 3 by showing transition from 1 m (Case 6) to 30 m (Case 5) at 250 Hz. At the intermediate source depth of 10 m, neither Case 1 nor Case 5 predicts the correct solution.

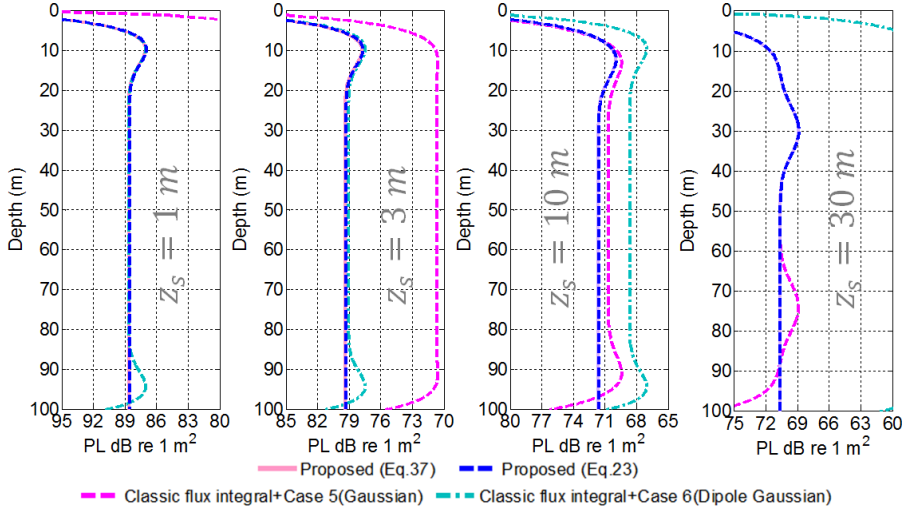


Figure 3. Propagation loss (PL) vs depth calculated by Eq.(23), Eq.(37) Weston's approach (Eq.(33)) for the different energy distribution with angle (Gaussian dipole Gaussian,) for different source depths (1 m, 3 m, 10 m and 30 m), Range is 25 km. Frequency is 250 Hz.

Eq.(33) and Eq.(35) each satisfy the reciprocity principle for their respective regime of applicability. For instance, Eq.(33) satisfies reciprocity for large receiver depths because of the use of $\sin^2(\gamma_{1n}z_s) \approx 1/2$ approximation. Eq.(35) satisfies reciprocity for sufficiently small source and receiver depth.

We apply Eq. (23) next (Figure 4) to investigate the depth dependence for Scenario A2.1 from the Weston Memorial Workshop, for frequencies in the range 50 Hz to 3500 Hz, at a range of 5 km. The symmetry approach described by Eq.(30) is used to obtain features close to the complementary depth and the seabed. The expressions for F_- and F_+ from Eq.(31) and Eq.(32) are evaluated numerically by the Rayleigh reflection coefficient based solution from Eq.(29), with and without beam shifts. There is good agreement with KrakenC, especially when the source or receiver is close to the sea surface. Although the results with the effect of beam shift are closer to KrakenC predictions than without beam shift, the difference is small. The beam shift can lead to larger differences especially for low frequencies. The proposed solution (Eq.(29)) can provide an accurate approximation to the incoherent normal mode sum, without the need to compute discrete eigenvalues.

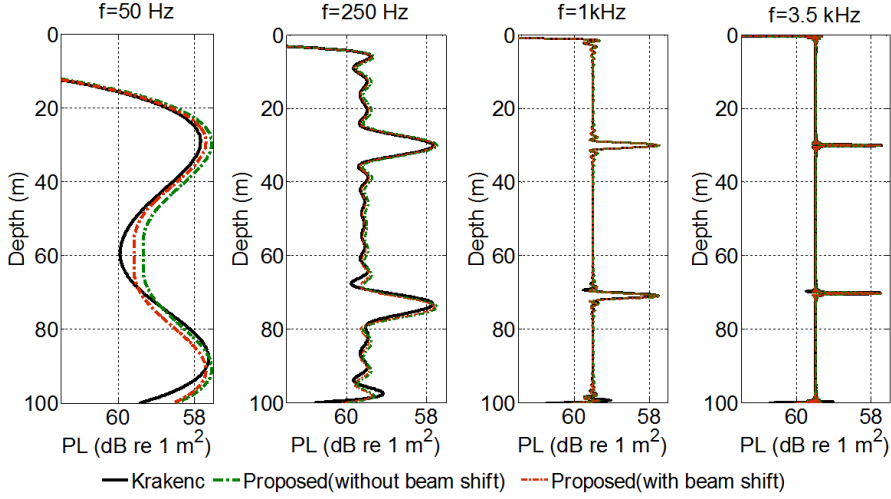


Figure 4. PL vs receiver depth by KrakenC and Eq. (30) (F_0 is calculated using Eq. (29)) for 50 Hz, 250 Hz, 1 kHz and 3.5 kHz at a range of 5 km from the source. The source depth is 30 m.

The classic flux integral without depth dependent properties (Eq. (34)) is selected as a reference PL ($PL_{\text{ref}} = 10 \log_{10} \frac{F_{\text{ref}}^{-1}}{1 \text{ m}^2} \text{ dB}$), with $h = 100 \text{ m}$, $\eta \cong 0.273777 \text{ Np/rad}$ and $\theta_c = 0.489957 \text{ rad}$. The relative PL ($PL_{\text{relative}} = PL - PL_{\text{ref}}$) is shown in Figure 5. PL is calculated using Eq.(30) (with the Rayleigh reflection coefficient, without beam shift) and KrakenC. In Figure 5, the range variation of the relative PL versus range at receiver depths 1 m, 30 m and 50 m is shown for 250 Hz. Good agreement between Kraken and Eq.(30) is observed. The largest differences between the proposed solution and Kraken at the different receiver depths considered are 0.19 dB (at 1 m), 0.07 dB at (30 m) and 0.15 dB (at 50 m). Figure 5 also shows the contribution of the proposed solution to Weston's classical flux integral. For example, we see large effects due to the surface decoupling at 1 m receiver depth.

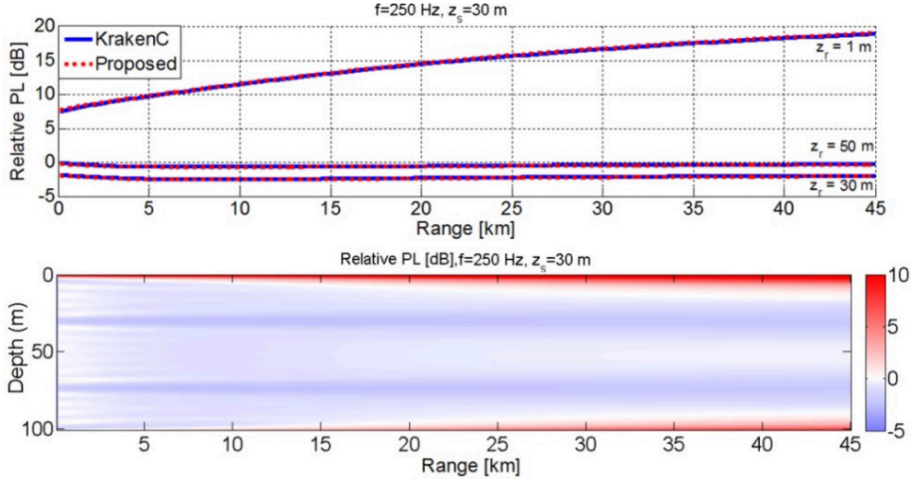


Figure 5. Relative Propagation loss ($PL_{relative} = PL - PL_{ref}$) versus range at different receiver depths (1 m, 30 m and 50 m) for 250 Hz (upper graph). Relative Propagation loss versus depth and range for 250 Hz (lower graph). PL is calculated using Eq.(30) (without beam shift) and KrakenC (incoherent mode sum). PL_{ref} is the reference PL from Eq. (34).

2.2.4. Conclusions

In this section, the depth dependence of propagation loss (PL) is investigated by deriving a depth-dependent correction term (as given by Eq.(19)) to the error function associated with the classical flux solution(Eq.(34)). This equation is derived from an incoherent normal mode sum, and provides a depth-dependent solution for a lossy Pekeris waveguide without the need for (computationally expensive) calculation of eigenvalues. Eq. (23) provides an analytical solution which includes all relevant depth corrections (Weston's low pass, Gaussian, and dipole Gaussian cases) in one formula. the depth dependence of PL for long ranges can be estimated by a simpler formula Eq.(37). If it is desired, a numerical solution based on Rayleigh reflection coefficient (Eq.(29)) including beam shifts can be also used in order to increase the accuracy. The explicit form of the result provides insight into the behaviour of the sound field close to the source depth, complementary source depth, sea surface and seabed.

APPENDIX A: THE SYMMETRY OF PROPAGATION FACTOR BY MODE SUM

The purpose of this appendix is to demonstrate that, if Weston's vertical wave shift is assumed to be independent of angle, the propagation factor for a source at the complementary source depth is equal to that for a source at the true source depth, and similarly for the receiver (for the isovelocity and isodensity case). Substituting $\gamma_{1n} = \frac{n\pi}{D}$ into

$$F(z_s, z_r) = \frac{2\pi}{r} \sum_{n=1}^{\infty} \frac{A_n^4 \sin^2(\gamma_{1n} z_r) \sin^2(\gamma_{1n} z_s)}{\kappa} \exp(-2\delta_n r) \quad (A.1)$$

the propagation factor becomes

$$F(z_s, z_r) = \frac{2\pi}{r} \sum_{n=1}^{\infty} \frac{A_n^4 \sin^2\left(n\pi \frac{z_s}{D}\right) \sin^2\left(n\pi \frac{z_r}{D}\right)}{\kappa_n} \exp(-2\delta_n r) \quad (A.2)$$

By using the periodicity property of trigonometric functions as $\sin^2\left(n\pi \frac{D-z_r}{D}\right) = \sin^2\left(n\pi \frac{z_r}{D}\right)$, the equation

$$F(z_s, D - z_r) = \frac{2\pi}{r} \sum_{n=1}^{\infty} \frac{A_n^4 \sin^2\left(n\pi \frac{z_s}{D}\right) \sin^2\left(n\pi \frac{z_r}{D}\right)}{\kappa_n} \exp(-2\delta_n r) \quad (A.3)$$

is obtained for the complementary receiver depth . The right hand side of this equation is equal to the propagation factor for z_r thus proving that the propagation factors at receiver and complementary receiver depths are equal. By repeating the same steps for the complementary source depth as $D - z_s$, a similar identity can be obtained. The resulting identities can be written

$$F(z_s, z_r) = F(z_s, D - z_r) \quad (A.4)$$

$$F(z_s, z_r) = F(D - z_s, z_r) \quad (A5)$$

and therefore

$$F(z_s, z_r) = F(D - z_s, D - z_r) \quad (A6)$$

These symmetry properties can be exploited to avoid the need to calculate PL for all receiver and source depth combinations separately. For computational efficiency, PL for all receiver depths can be calculated by Eq.(30) which based on these properties.

APPENDIX B: THE ASYMMETRY OF PROPAGATION FACTOR BY INTEGRAL SOLUTION

In this section, the symmetry of the integral representation is investigated. Figure 2 demonstrates that the integral over a continuum of modes fails to exhibit the symmetry property of the discrete mode sum characterised by Eq.(A4)-Eq.(A5). the purposes of this Appendix are to describe the conditions for which the integral solution breaks down and explain the reason for this failure. The differences between the discrete mode summand and continuous angle integrand are also shown. the $W(z_r, z_s, \theta)$ term in the integral solution is derived from eigenfunctions, which lead to the symmetrical propagation factor as described in Appendix A. First, the symmetry of $W(z_r, z_s, \theta)$ is investigated by replacing z_r with $-z_r$:

$$\begin{aligned} & W(D - z_r, z_s, \theta) \\ &= \cos(2z_s k_1 \sin \theta) + \cos(2Dk_1 \sin \theta - 2z_r k_1 \sin \theta) \\ &= \frac{\cos(2(z_s + z_r)k_1 \sin \theta - 2Dk_1 \sin \theta) + \cos(2(z_s - z_r)k_1 \sin \theta + 2Dk_1 \sin \theta)}{2} \end{aligned} \quad (B1)$$

The symmetry property shown by Eq.(A5) and Eq.(A6) comes from the periodicity of trigonometric functions. Thus, in order to ensure the symmetry property, $2Dk_1 \sin \theta$ must be equal to $2n\pi$, which holds only for the discrete angles corresponding to the eigenvalues. However, this relation is not valid for the non-integer values of n (continuous angles). Thus, having continuous angles in the integration can cause an asymmetric solution. The following equality can only be written for the discrete angles (θ_n),

$$\gamma_n = k_1 \sin(\theta_n) = \frac{n\pi}{D}, n = 1, 2, 3, \dots \quad (B2)$$

Eq.(B1) and Eq.(18) for continuous angles are different. This means the symmetry relations formulated by Eq.(A4) to Eq.(A6) are not satisfied for the continuous angle approximation. For an illustration of symmetry properties for discrete and continuous angles, the argument of $\sin^2(\gamma_n z_r) \sin^2(\gamma_n z_s)$ is plotted for discrete eigenvalues ($\gamma_n = \frac{n\pi}{D}$) and continuous angles ($\gamma_n = k_1 \sin \theta$) in Figure 6. The same comparison is also repeated for the complementary receiver depth as $\sin^2(\gamma_n (D - z_r)) \sin^2(\gamma_n z_s)$. The symmetry property for the receiver (Eq.(A4)) requires $\sin^2(\gamma_n z_r) \sin^2(\gamma_n z_s) = \sin^2(\gamma_n (D - z_r)) \sin^2(\gamma_n z_s)$. The validity of the continuous angle approach is investigated by the comparisons in Figure 6. For this comparison, $f = 250$ Hz, $z_r = 10$ m, $D = 104.06$ m and $\theta_c = 0.49$ rad .

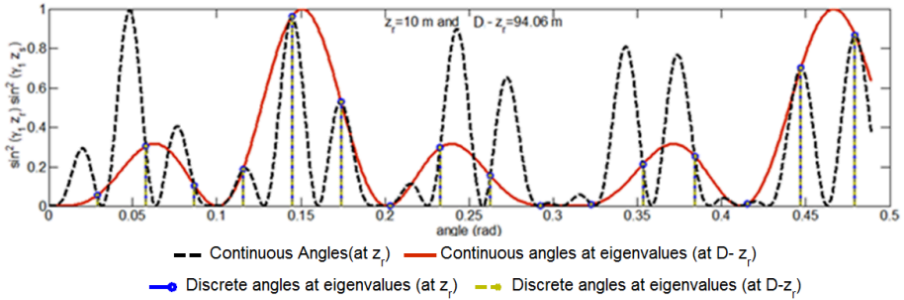


Figure 6. Variation of $\sin^2(\gamma_n z_r) \sin^2(\gamma_n z_s)$ for discrete angles at eigenvalues (vertical bars) and continuous angles (solid and dashed lines). the source depth is 30 m.

This comparison shows that the discrete mode solutions at receiver depth and complementary receiver depth are identical when calculated using Weston's wave shift concept, if the vertical wave shift is assumed independent of grazing angle. According to Eq. (B2), the discrete angles are calculated as $\theta_n = \arcsin\left(\frac{nc_1}{2Df}\right)$. The continuous angles can be any value between zero and θ_c , irrespective of the eigenvalues. In order for the continuous angle integral to approximate the discrete mode sum, the area under the curves in Figure 6 must be equal to the sum of contributions from discrete eigenvalues, which is the case if the curve contains no energy above

the Nyquist frequency corresponding to the rate at which the curves are sampled by the series of eigenvalues. Writing

$$\sin\left(\frac{n\pi}{D}z_s\right)\sin\left(\frac{n\pi}{D}z_r\right) = \frac{1}{2i}\left(\exp\left(i\frac{n\pi}{D}z_s\right) - \exp\left(-i\frac{n\pi}{D}z_s\right)\right)\frac{1}{2i}\left(\exp\left(i\frac{n\pi}{D}z_r\right) - \exp\left(-i\frac{n\pi}{D}z_r\right)\right),$$

the highest frequency component is the term proportional to $\exp(\pm i2n\pi F)$, where the highest frequency, F , is equal to $\frac{z_s+z_r}{2D}$. According to the Nyquist-Shannon theorem, the continuous function is well sampled, in the sense that it can be reconstructed from these samples, by the discrete modes if F is less than the Nyquist frequency (half the sampling rate), which is equal to 0.5. While it does not follow directly from this theorem, it seems reasonable to assume that the integral of a continuous function will be a good approximation to a discrete sum if the maximum frequency is below the Nyquist frequency corresponding to the sampling rate, and not otherwise. If the continuous function is sufficiently well sampled in the same sense, one can therefore expect the integral to exhibit the same symmetry property as the discrete sum. Given that the maximum frequency is $F = \frac{z_s+z_r}{2D}$ and the Nyquist frequency is 0.5, it follows that the condition for symmetry is $z_s+z_r < D$. This condition shows that the proposed solution is valid up to the complementary source depth ($z_r < z_{cs}$). Thus, the proposed solution by the continuum approach is valid for $z_r < z_{cs} - 2\sigma$, where σ is the width of the peak at the complementary source depth. In the mode stripping, this width is given by the simple formula as $\sigma = \frac{1}{2k_1\phi_0}$. In the cylindrical spreading region, the width is less well defined.

Even though the symmetry properties are not satisfied for the integral representation at the complementary source and receiver depths, the correct propagation factor can be obtained by exploiting the symmetry of Eq.(30) for $D/2 < z_r < D$.

APPENDIX C: DERIVATIONS OF WESTON'S CASES 5 AND 6 FROM THE PROPOSED SOLUTION

In this Appendix, Weston's Case 5 (Gaussian) and Case 6 (dipole Gaussian) are derived from Eq.(37).

Derivation of Case 5

When z_s is large enough and far from the waveguide's boundaries ($k_1 z_s \phi_0 \gg 1$, such that $\exp(-2(k_1 z_s \phi_0)^2)$) may be neglected, the propagation factor can be written as

$$F_0(z_r, z_s) \approx F_{\text{ref}}(1 - \exp(-2(k_1 z_r \phi_0)^2)) \quad (C1)$$

consistent with Weston's Case 5. Eq.(C1) can also be derived from [Denham,1986] by applying the reciprocity principle to Eq. (25) from that paper.

Derivation of Case 6

When z_s is small and close to sea surface, the propagation factor can be written as

$$F_0(z_r, z_s) = F_{\text{ref}}(1 - \exp(-2\varepsilon^2) - \exp(-2(k_1 z_r \phi_0)^2) [1 - \exp(-2\varepsilon^2) \cosh(4k_1 z_r \phi_0 \varepsilon)]) \quad (C2)$$

Where $\varepsilon = k_1 z_s \phi_0$. For small ε , the exponential and hyperbolic cosine function can be replaced with $\exp(-2\varepsilon^2) \approx 1 - 2\varepsilon^2$ and $\cosh(4\varepsilon k_1 z_r \phi_0) \approx 1 + \frac{(4\varepsilon k_1 z_r \phi_0)^2}{2} = 1 + 8(\varepsilon k_1 z_r \phi_0)^2$,

$$F_0(z_r, z_s) = F_{\text{ref}}(2\varepsilon^2 - \exp(-2(k_1 z_r \phi_0)^2)[1 - (1 - 2\varepsilon^2)(1 + 8(\varepsilon k_1 z_r \phi_0)^2)]) \quad (C3)$$

Then, neglecting terms of order ε^4 or higher

$$F_0(z_r, z_s) = 2\varepsilon^2(1 - (1 - 4(k_1 z_r \phi_0)^2)\exp(-2(k_1 z_r \phi_0)^2))F_{\text{ref}} \quad (C4)$$

consistent with Weston's Case 6. For large receiver depths, this expression may be approximated using $\exp(-2(k_1 z_r \phi_0)^2) \approx 0$, in which case Eq. (27) from [Denham,1986] is recovered.